The EMBO Journal Vol. 19 No. 22 pp. 5951–5961, 2000

Crystal structure of MalK, the ATPase subunit of the trehalose/maltose ABC transporter of the archaeon *Thermococcus litoralis*

Kay Diederichs, Joachim Diez, Gerhard Greller, Christian Müller[1], Jason Breed[2], Christoph Schnell, Clemens Vonrhein[3], Winfried Boos and Wolfram Welte[4]

Fachbereich Biologie, Universität Konstanz, M656, D-78457 Konstanz, Germany, [1]School of Bioscience, Cardiff University, 10 Museums Avenue, PO Box 911, Cardiff CF10 3US, [2]Astra Zeneca, Mereside, Macclesfield SK10 4TG and [3]Global Phasing Ltd, Sheraton House, Castle Park, Cambridge CB3 0AX, UK

[4]Corresponding author
e-mail: wolfram.welte@uni-konstanz.de

The members of the ABC transporter family transport a wide variety of molecules into or out of cells and cellular compartments. Apart from a translocation pore, each member possesses two similar nucleoside triphosphate-binding subunits or domains in order to couple the energy-providing reaction with transport. In the maltose transporter of several Gram-negative bacteria and the archaeon *Thermococcus litoralis*, the nucleoside triphosphate-binding subunit contains a C-terminal regulatory domain. A dimer of the subunit is attached cytoplasmically to the translocation pore. Here we report the crystal structure of this dimer showing two bound pyrophosphate molecules at 1.9 Å resolution. The dimer forms by association of the ATPase domains, with the two regulatory domains attached at opposite poles. Significant deviation from 2-fold symmetry is seen at the interface of the dimer and in the regions corresponding to those residues known to be in contact with the translocation pore. The structure and its relationship to function are discussed in the light of known mutations from the homologous *Escherichia coli* and *Salmonella typhimurium* proteins.

Keywords: active transport/CFTR/crystal structure/maltose uptake and regulation/P-glycoprotein

Introduction

ABC transporters are found in all eubacterial, archaeal and eukaryotic species studied to date and most probably represent the largest family of homologous proteins. In *Escherichia coli*, an estimated 5% of the whole genome encodes them (Linton and Higgins, 1998).

ABC transporters are modular mechanical machines that couple ATP hydrolysis to the physical movement of molecules through membranes. Several subclasses can be defined according to the direction of substrate translocation, substrate specificity and subunit organization. Prominent family members are P-glycoprotein involved in multiple drug resistance, the gated chloride channel cystic fibrosis transmembrane conductance regulator (CFTR) involved in the inherited disease cystic fibrosis, sterol transporters, eye pigment precursor importers and protein exporters. Even though the array of substrates seems endless and the molecular architecture can be rather diverse, the ATPase module is an essential and conserved subunit of all transporters. Its sequence features are the main basis for the identification of new family members (Holland and Blight, 1999).

A subfamily of ABC transporters are binding protein-dependent systems that are ubiquitous in eubacteria and archaea, where they catalyse the high-affinity uptake of small polar substrates into the cell. One of the best studied examples is the *E.coli* maltose–maltodextrin system (Boos and Lucht, 1996; Boos and Shuman, 1998). It consists of a binding protein (MalE) as its major substrate recognition site, located in the periplasm. Two homologous hydrophobic membrane proteins (MalF and MalG) form a heterodimeric translocation pore with a dimer of the ATP-hydrolysing subunit (MalK) associated from the cytoplasmic side. Formation of the $MalEFGK_2$ transport complex therefore couples ATP hydrolysis with active transport of substrate.

The *E.coli* MalK (E.c.MalK) and its *Salmonella typhimurium* homologue (S.t.MalK), which share 95% identical residues, have been subject to intense analysis ever since their discovery (Bavoil *et al*., 1980; Shuman and Silhavy, 1981). Studies of enzymatic activity as an ATPase (Morbach *et al*., 1993; Davidson *et al*., 1996) have been performed. The homodimeric subunit interaction has been analysed (Davidson and Sharma, 1997; Kennedy and Traxler, 1999), and the requirements for its assembly in the transport complex (Davidson and Nikaido, 1991; Panagiotidis *et al*., 1993; Lippincott and Traxler, 1997) have been recognized. Mutational analysis for domain interactions with its cognate membrane components (Mourez *et al*., 1997) as well as cross-linking studies (Hunke *et al*., 2000a) have been reported. Mutational analysis has also defined the functional importance of conserved regions such as Walker-A, Walker-B and the switch region for ATP binding, as well as the signature motif region and the helical domain for coupling of ATP hydrolysis to transport (for a review see Schneider and Hunke, 1998), and has revealed a remarkable versatility of MalK to interact with different regulatory proteins. According to other studies, MalK is able to interact with unphosphorylated $EIIA^{Glc}$, a subunit of the phosphotransferase (PTS)-type glucose transporter, leading to the inhibition of maltose transport (Dean *et al*., 1990; Vandervlag and Postma, 1995), a phenomenon called inducer exclusion. In addition, the C-terminus of MalK is able to affect *mal* gene regulation (Kühnau *et al*., 1991) by interacting with and inactivating MalT, the specific gene activator of *mal* gene expression (Panagiotidis *et al*.,

Table I. Statistics on data reduction and MAD phasing for MalK data sets

	Native	$HgCl_2$			
		peak	inflection	remote high	remote low
Wavelength (Å)	0.8424	1.0080	1.0089	1.0163	1.0000
Resolution[a] (Å)	1.86 (1.88–1.86)	2.65 (2.68–2.65)	2.65 (2.68–2.65)	2.65 (2.68–2.65)	2.65 (2.68–2.65)
Redundancy[a]	4.6 (3.0)	4.0 (4.0)	4.0 (4.1)	4.0 (3.2)	4.0 (4.1)
No. of unique observations[a]	82 668 (2430)	29 141 (963)	29 172 (965)	29 158 (934)	29 183 (963)
Completeness (%)	99.0 (93.8)	99.0 (99.8)	99.1 (100.0)	99.0 (96.8)	99.1 (99.8)
R-meas[b]	3.9 (28.0)	4.2 (13.9)	4.1 (16.3)	4.0 (17.5)	4.0 (15.8)
R-mrgd-F[b]	4.1 (27.2)	3.7 (10.8)	3.8 (12.9)	4.0 (15.8)	3.8 (12.2)
Isomorphous phasing power (acentric reflections)	–	–	5.61	6.45	3.41
Anomalous phasing power (acentric reflections)	–	1.88	1.23	1.13	0.25
Figure of merit	–	0.69			

[a]The values for the highest resolution shell are given in parentheses.
[b]*R*-mrgd-F as defined by Diederichs and Karplus (1997).

1998), demonstrating a link between transport of substrate and gene regulation.

Binding protein-dependent ABC transporters have also been found in thermophilic bacteria (Herrmann *et al*., 1996; Sahm *et al*., 1996). Recently, we described an ABC transporter for maltose/trehalose in the hyperthermophilic archaeon *Thermococcus litoralis* (Xavier *et al*., 1996). This transport system has several unusual properties: it shows a high affinity (K_m of ~20 nM) at 85°C, the optimum growth temperature of this organism, and it recognizes its very different substrates, maltose and trehalose, with equal affinity but does not bind larger maltodextrins. Its cognate binding protein has been purified (Horlacher *et al*., 1998) and its crystal structure has been solved (J.Diez, K.Diederichs, G.Greller, R.Horlacher, W.Boos and W.Welte, manuscript submitted). The *T.litoralis* MalK (T.l.MalK) has been heterologously expressed in *E.coli* and its biochemical properties have been studied. Its sequence, size (372 residues) and biochemical properties reveal its close relationship to the E.c.MalK protein. It optimally hydrolyses ATP at 85°C and exhibits a K_m of 150 μM for ATP at this temperature (Greller *et al*., 1999).

Little is known about how ATP hydrolysis, presumably via a series of protein conformational changes (Ehrmann *et al*., 1998), is coupled to the mechanism of transport. Thus, structural information about the translocating complex as well as the ATP-coupling structures is needed. As to the subclass of importers, the only known atomic structure is that of HisP, the ATP-hydrolysing subunit of the histidine transporter of *S.typhimurium* (Hung *et al*., 1998).

Here we present the crystal structure of T.l.MalK, the energy-coupling subunit of the trehalose/maltose transporter of *T.litoralis*, at 1.9 Å resolution.

Results

Purification and crystal structure analysis of T.l.MalK

Instead of a C-terminally His-tagged T.l.MalK as published previously (Greller *et al*., 1999), we constructed an N-terminally His-tagged MalK that appeared to crystallize more easily. The recombinant protein was purified from the soluble cellular extract of strain BL21, which lacks several proteases (Studier and Moffatt, 1986), as described previously. The ATPase activity corresponded to that of the previously published construct containing a C-terminal His tag.

The crystals comprise two molecules (termed A and B) per asymmetric unit, and the structure was solved by multiwavelength anomalous diffraction (MAD) analysis of an $HgCl_2$ derivative. As only one atom of Hg per molecule of MalK was bound, the phasing power was low. Furthermore, despite cryogenic conditions, the isomorphous and anomalous signal strongly decreased with exposure time, presumably due to radiation damage. The crystallographic analysis therefore first employed single anomalous diffraction (SAD) phasing at the peak wavelength, and was then extended to include all four wavelengths. To stabilize the heavy atom refinement process in the four-wavelength case, the Hendrickson–Lattman coefficients of the SAD phases were introduced as external restraints. The phasing power values given by SHARP (de la Fortelle and Bricogne, 1997; Table I) are much higher for the isomorphous than for the anomalous signal, which is atypical for a MAD experiment and is more reminiscent of a multiple isomorphous replacement (MIR) analysis.

After initial automatic ARP/wARP (Lamzin and Wilson, 1993) model building, model refinement was continued using standard procedures at 1.9 Å.

Although T.l.MalK was crystallized in the presence of ADP, there was only clear density for a pyrophosphate molecule. At the expected position of the adenosine group, the map shows elongated density that could result from superposition of several adenosine groups. The occupancy of the pyrophosphate was determined as 0.7. The missing density for the nucleoside can thus be attributed to disorder and low occupancy. Obviously, the structure deviates from the ATP-binding conformation.

Comparison with known structures

Comparison of the structures of the ATPase domain of T.l.MalK and HisP reveals an almost identical fold (for

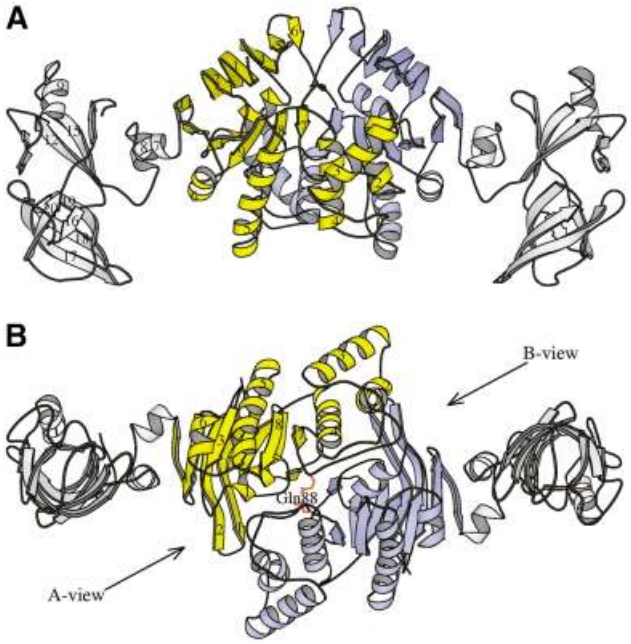

Fig. 1. Ribbon representation of the T.l.MalK dimer. The A- and B-molecules are coloured yellow and blue, respectively, except for both regulatory domains which are coloured grey. Labels indicate the numbers of strands and helices according to the secondary structure assignment given in Figure 3. This figure and the following structural diagrams were made with MOLSCRIPT (Kraulis, 1991) if not indicated otherwise. (**A**) The side view shows the extended dumb-bell shape resulting from the two regulatory domains on either end and the central ATPase domain dimer. The pseudo 2-fold symmetry axis is oriented vertically and runs through the centre of the dimer. The strong involvement of helices 2 and 4 in dimerization is seen. The bottom part of the dimer is supposed to interact with the membrane translocation pore MalFG. (**B**) The bottom view along the pseudo 2-fold axis shows the deviation from 2-fold symmetry. The helical layer of one monomer is seen in contact with the two upper layers containing the nucleotide-binding site of the other monomer. Gln88 residues from both monomers are shown to demonstrate their close apposition. The A- and B-viewing directions are indicated.

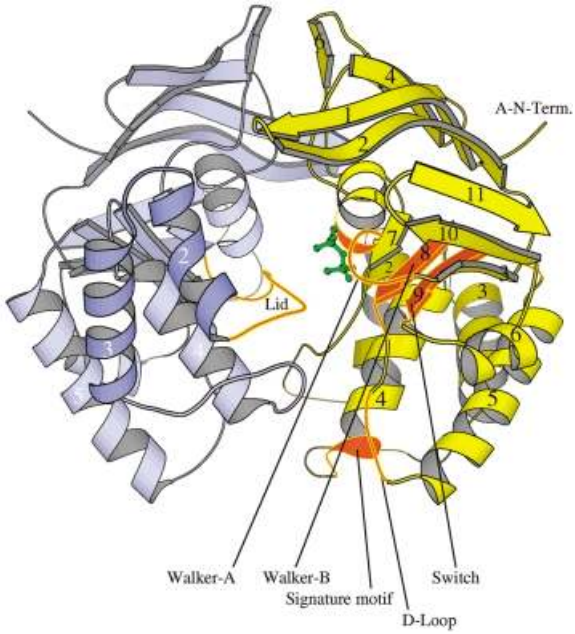

Fig. 2. A-view along the interface perpendicular to the pseudo-symmetry axis. From top to bottom the three layers are seen: antiparallel sheet; mixed sheet with a P-loop; and helix 1 and helical layer. Colouring is as in Figure 1 except that the conserved regions Walker-A, Walker-B, signature motif, D-loop, switch from monomer A and the 'lid' region from monomer B are marked by red colouring with yellow outlines. Labels indicate the numbers of strands and helices according to the numbering given in Figure 3.

the A and the B monomer, r.m.s.d. values of 1.71 Å for 153 C_α-coordinates and 1.95 Å for 206 C_α-coordinates at a cut-off of 3.8 Å were found, respectively). The only significant difference is an additional helix–strand motif after strand 7 in HisP as compared with T.l.MalK.

Rad50 is a protein involved in DNA double strand repair and is found in all kingdoms of life. It forms a heterodimer with its N- and C-terminal fragments, termed Rad50cd (Hopfner *et al*., 2000), which, upon binding of ATP, dimerizes with another Rad50cd heterodimer and becomes active as an ATPase. Rad50cd shares the homology regions with ABC-type ATPases and is structurally similar to the monomers of T.l.MalK and HisP, although the r.m.s.d. values are much higher than between the latter. With respect to the mode of dimerization, all three published structures differ from each other so that in contrast to the view of Hopfner *et al*. (2000), the Rad50cd dimer cannot be used as a model for the nucleotide-binding domains of ABC transporters.

General description of the structure

T.l.MalK consists of two domains. The N-terminal 223 residues form an α/β-type ATPase domain as found in the ABC transporter family (Armstrong *et al*., 1998; Hung *et al*., 1998; Linton and Higgins, 1998). Its overall shape resembles an ellipsoidal planeconvex lens with a longer (~55 Å) and a shorter (~40 Å) axis. Residues 224–372 (regulatory domain) form a barrel with a diameter of ~20 Å and a height of 45 Å.

In the asymmetric unit, the ATPase domains of two adjacent MalK molecules are apposed with part of their flat faces to form a globular dimer with significant deviations from 2-fold symmetry (Figure 1). Attached to opposite poles of the dimer are the regulatory domains, resulting in an extended dumb-bell-shaped molecule with a long axis of ~120 Å. In the following, the bottom and top of T.l.MalK will be referred to on the basis of the orientation given in Figure 1A. As will be shown later, the bottom part contains the residues involved in interaction with MalFG. The contact interface between the ATPase domains extends along the 2-fold axis and forms an angle of ~35° with the long axis of the dimer (see Figure 1B). When viewed along the interface perpendicular to the pseudosymmetry axis, the ATPase domains are composed of three layers (Figure 2). An antiparallel β-sheet formed by strands 2, 1, 4, 5 and 6 forms the top layer (see Figure 3 for the numbering of the secondary structure elements). The middle layer contains a mixed β-sheet formed by the parallel strands 10, 3, 9, 8 and 7, and the antiparallel strand 11, which connects to the regulatory domain. A final and essential part of the middle layer is the P-loop and helix 1, which follow strand 3 and contain the Walker-A motif. They are located between the two sheets. The P-loop contains a pyrophosphate molecule bound at the interface. Comparison with the similar ATPase structures

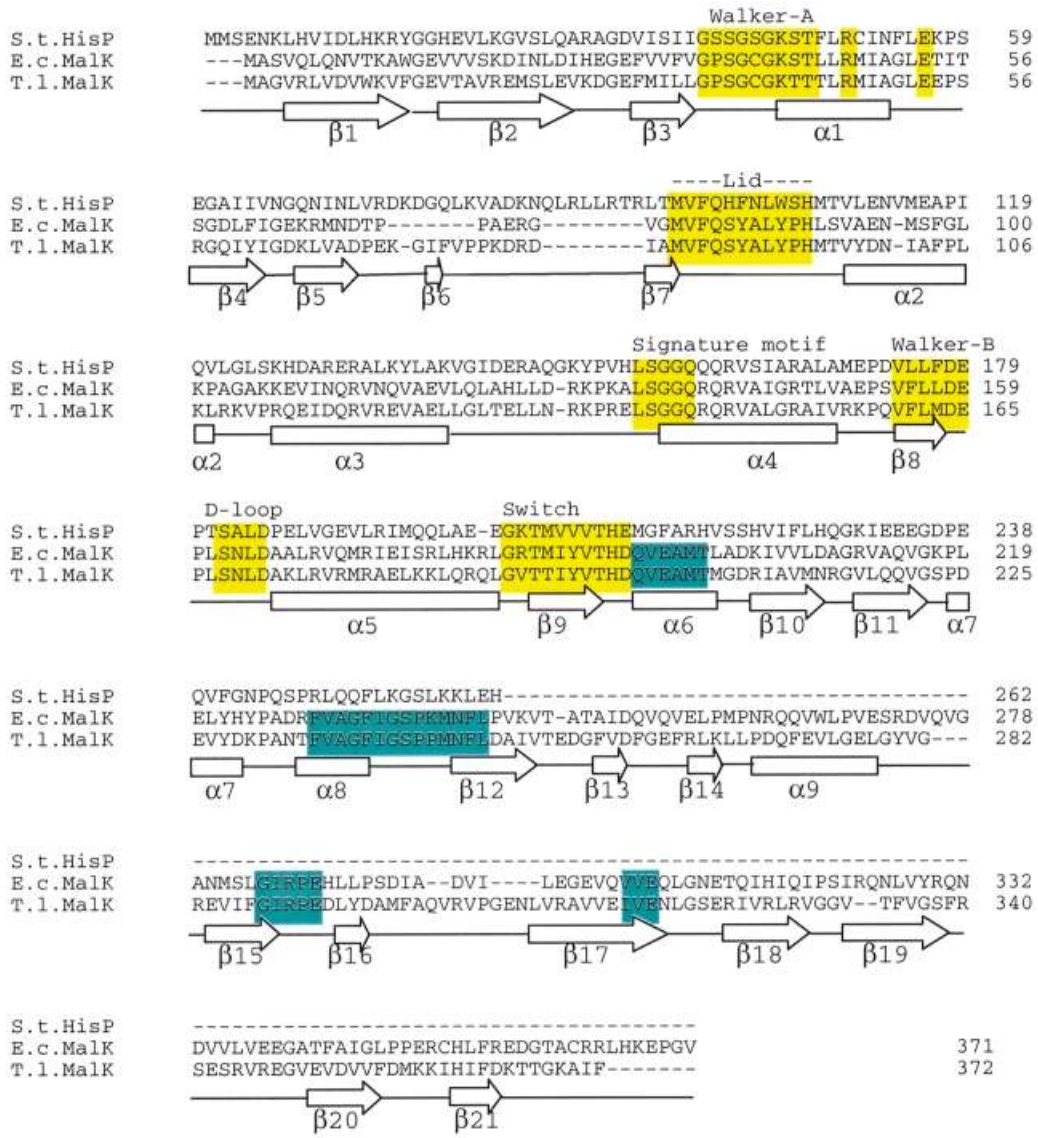

Fig. 3. Structural alignment of HisP from *S.typhimurium* (Hung *et al*., 1998) and of T.l.MalK, as well as sequence alignment with E.c.MalK. Secondary structure elements of T.l.MalK are indicated and numbered. Regions that are conserved in all three sequences are shaded yellow, those that are conserved only between the two MalKs are shaded blue.

of HisP and Rad50cd complexed with ATP (Hung *et al*., 1998; Hopfner *et al*., 2000) shows that the two phosphates are positioned similarly to the α and β phosphates of ATP. The two sheets of the upper two layers approach each other at roughly a right angle. The last and bottom layer consists of helices 2–6, of which helices 2 and 4 form most of the interface with the other ATPase domain (Figure 1).

We find that the majority of the regions conserved in ABC-type ATPases, i.e. the Walker-A, the Walker-B and the switch region (Linton and Higgins, 1998; Schneider and Hunke, 1998; Hopfner *et al*., 2000), are placed around the pyrophosphate group in or near the parallel sheet of the middle layer (Figure 2). Two conserved regions that contain residues known to be involved in interaction with the translocation pore MalFG are at the bottom of the helical layer (signature motif and D-loop). Another less well conserved region is around a highly conserved glutamine residue at position 88 in T.l.MalK. Hopfner *et al*. (2000) have used the term 'Q-loop' for this region, while we prefer the descriptive term 'lid' in order to convey its location near the nucleotide-binding site (Figure 2).

The MalK dimer

Given the two non-crystallographic MalK molecules in the $P2_12_12$ crystal lattice, several choices of dimers are possible in principle. One rationale to select the biologically relevant dimer was that it should bury a large surface area from solvent. When arranging the buried surfaces of possible dimers in decreasing order, the four largest values are 2755, 1715, 1075 and 719 Å^2. In none of these does the arrangement of the nucleotide-binding domains resemble the proposed dimer of HisP (Hung *et al*., 1998). Furthermore, the dimer with the largest buried surface is in accord with other data, as will be discussed below. We therefore strongly favour this dimer, although it is different from that proposed for HisP, which buries 915 Å^2, and from that of Rad50cd (Hopfner *et al*., 2000), which buries 2631 Å^2.

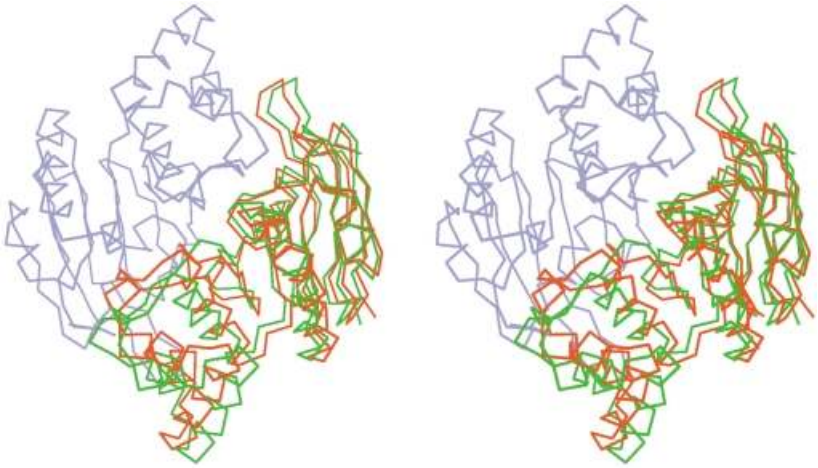

Fig. 4. Stereo bottom view (C_α chain) of the ATPase domain dimer. The A- and B-chains are coloured green and blue, respectively. The B-chain has been superimposed with the A-chain and is shown in red. The good matching of the sheets in the upper two layers is seen, while helices 2–4 are shifted against each other.

Although the T.l.MalK dimer interface is formed by many apolar residues (22), mainly with aromatic side chains (10), there are a majority of polar residues (29). Interestingly, there is no direct intermolecular hydrogen bond. The cavities in the interface and the immobilized solvent molecules (25) indicate that the interaction energy is not predominantly hydrophobic.

Deviations from 2-fold symmetry

Inspection of Figure 1B shows that the A-regulatory domain can be superimposed with its B-domain partner by a clockwise rotation of ~170° around the pseudo 2-fold axis. A least squares superposition of the ATPase domains with a cut-off of 3.8 Å superimposes 200 C_α atoms with an r.m.s.d. value of 1.7 Å (Figure 4). While the sheets closely match each other, significant displacements are found for the loop between strand 7 and helix 2 (containing the 'lid' region) as well as for helices 2 and 3. The latter are shifted in the B-monomer by up to 3 Å outwards compared with the corresponding helices of the A-monomer (see Figure 4). Thus, the upper and middle layer, upon a rotational displacement from ideal 2-fold symmetry, appear to behave virtually as a rigid structure rotating around the pseudo 2-fold axis, while the helices (notably helices 2 and 3) show conformational plasticity of the interface.

The asymmetry is also obvious when the dimer is viewed upright in two opposite directions along an axis oriented perpendicular to the 2-fold axis and along the interface (Figures 1B and 5). We distinguish between the A-view, which has the A-monomer on the right and the B-monomer on the left, and the B-view, with the two monomers arranged oppositely. In the A-view (Figure 5A), the interface appears more narrow as B-His95 Nδ1 of the 'lid' region approaches an oxygen of the β-phosphate of the A-pyrophosphate to within hydrogen-bonding distance (Figure 6). In the B-view (Figure 5B), the 'lid' of the A-molecule is seen to be shifted by ~6 Å towards the bottom, thus opening the interface and interrupting the interaction of the B-His with the pyrophosphate. This shift brings A-Tyr93 OH of the 'lid' within hydrogen-bonding distance of another β-phosphate-bonded oxygen from B-pyrophosphate (Figure 6); this proximity is absent in the A-view. Due to the high *B*-factors in this region (Figure 7), a hydrogen-bonding distance is not satisfactory evidence for existence of the bond.

Lys42, which is highly conserved among nucleoside triphosphate-binding proteins, also shows slight asymmetry with respect to its Nε hydrogen bonds with the phosphate oxygens of the β-phosphate of the pyrophosphate molecule due to an altered side chain conformation. While in the B-molecule one oxygen is within hydrogen-bonding distance, in the A-molecule there are two oxygens (Figure 6).

Arg47 shows two different side chain conformations. In the A-molecule, it forms a salt bridge with A-Glu53. In contrast, in the B-molecule, a hydrogen bond between the NH_2 group and the Oγ1 of B-Thr44 is formed (Figure 6). All three residues are conserved in HisP, E.c.MalK and T.l.MalK (Figure 3).

The distances between the C_α atoms of Glu139 in the conserved signature motif at the bottom end of helix 4 and of Leu170 in the conserved D-loop motif near the bottom (Figures 1B, 2 and 3) provide another example for the deviation from 2-fold symmetry. While A-Glu139C_α and B-Leu170C_α are 13.6 Å apart, the distance between B-Glu139C_α and A-Leu170C_α is only 8.8 Å.

Furthermore, the deviations from 2-fold symmetry manifest themselves in the *B*-factors (Figure 7). The 'lid', the loop between the two asymmetric helices 2 and 3 and the signature motif at the N-terminal end of helix 4 near the bottom have significantly higher values in the A- than in the B-monomer.

The regulatory domain

The regulatory domain contains the 149 C-terminal residues of T.l.MalK, which form a small connecting domain of 22 residues (helices 7 and 8), an antiparallel sheet of three β-strands and a five-stranded β-barrel with shear number 10 (see Figures 1A and 3).

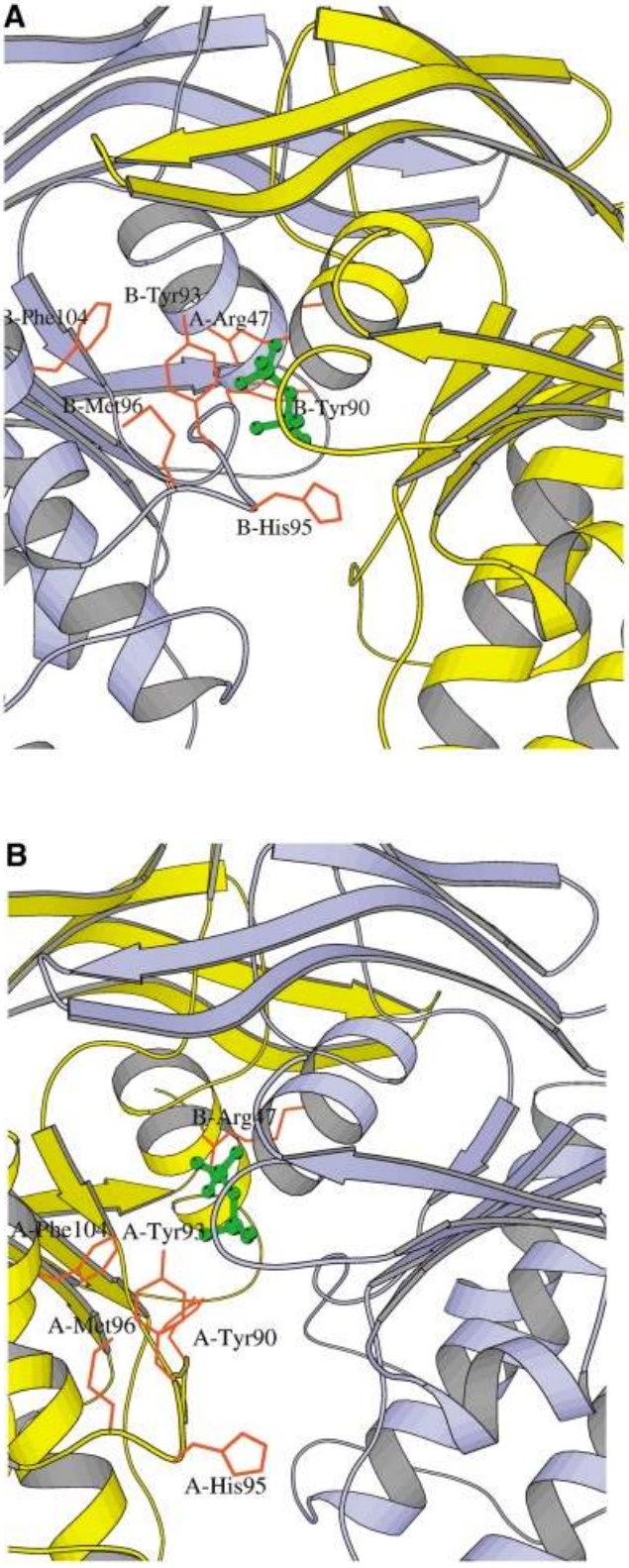

Fig. 5. Comparison of the A- and B-view. In the A-view (**A**), the interface appears to be more narrow than in the corresponding B-view (**B**) due to the upward shift of the loop containing the 'lid' region, which has been clarified by including side chains of residues 90, 93, 96 and 104. Notably, B-His95 approaches the pyrophosphate to within hydrogen-bonding distance in the A-view, while A-Tyr93 plays this role in the B-view. Arg47 shows a difference in side chain conformation in the two views. Helices 2 and 3 are shifted outwards in the B-monomer by ~3 Å as compared with the A-monomer.

A structure-based search using the DALI-server (Holm and Sander, 1993) indicated a weak similarity to an N-terminal fragment of phenylalanyl-tRNA and aspartyl-tRNA synthetases. Less similarity of the barrel also exists to the C-terminal aminoacyl-tRNA-binding domains of bacterial elongation factors EF-Tu (Kjeldgaard and Nyborg, 1992; Nyborg *et al*., 1996), the C-terminal barrel domain of bacterial methionyl-tRNA formyltransferase (Schmitt *et al*., 1996) and other proteins of the so-called OB-fold (Murzin, 1993). These domains function as binding modules for aminoacyl-tRNA, carbohydrates and DNA. In EF-Tu, they are connected to a nucleoside triphosphatase domain, a combination reminiscent of MalK.

The sequences of the regulatory domains of T.l.MalK and E.c.MalK are not very similar except for a region in the connecting domain and another between strands 15 and 16 (Figure 3). This is in accordance with the fact that interactions with regulatory proteins such as MalT and $EIIA^{Glc}$ are unknown in *T.litoralis*. The existence of the C-terminal domain in T.l.MalK indicates, however, that the ATPase is also involved in regulatory circuits. Indirect evidence for a similar fold of both regulatory domains are the few conserved regions that are shared by a larger number of members of the bacterial ABC-type ATPase domains, which also possess an extension of ~110 residues at the C-terminus of their ATPase domain. In S.t.MalK, the regulatory functions have indeed been mapped roughly to a segment of 106 residues at the C-terminus (Schmees and Schneider, 1998).

Discussion

The T.l.MalK dimer is in accord with restrictions by other data relevant for the dimer structure

The A85C mutant of S.t.MalK has been shown, under *in vitro* conditions (i.e. reconstituted with MalFG in liposomes), to form a disulfide-linked dimer by forming a bond between the two pseudosymmetry-related cysteines (Hunke *et al*., 2000a). This means that the backbones of both monomers in the vicinity of this residue must approach each other in the dimer interface to a distance of less than ~6 Å. In T.l.MalK, the alanine residue is conserved and corresponds to residue Ala91 in the 'lid' region. A-Ala91 and B-Ala91 are placed 17 Å apart. However, the 'lid' region has high and asymmetric *B*-factors (80 and 50 $Å^2$ for the A- and B-chains, respectively; Figure 7), and the backbones of the two T.l.MalK monomers at another nearby residue, Gln88, are indeed placed only 8.5 Å apart (Figure 1B). This shows that the T.l.MalK dimer can meet the strong distance restraint of the cross-linking result after a subtle structural rearrangement, and thus provides evidence that the crystal structure is close if not identical to one conformation of the MalK dimer in the transport complex.

Gln88 is conserved in most of the ABC-type ATPase domains (Schneider and Hunke, 1998). Among these are the two nucleotide-binding domains of the cystic fibrosis-related gated chloride channel CFTR. According to Hopfner *et al*. (2000) and Hung *et al*. (1998), it may coordinate Mg^{2+} and the water molecule that attacks the γ-phosphate bond. In our structure, the glutamine residues are placed too far away from the nucleotides to suggest

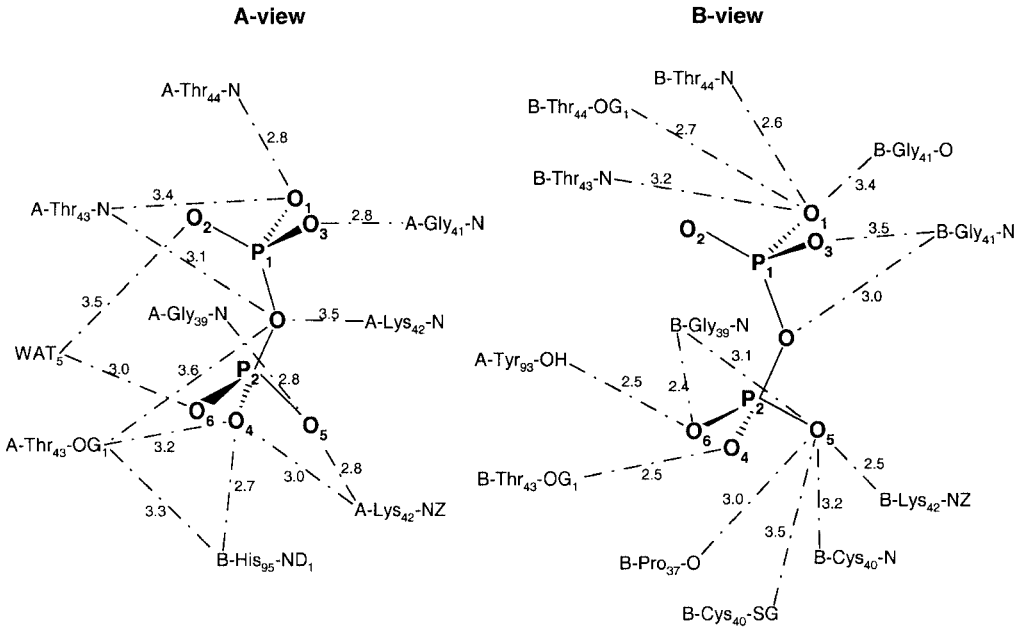

Fig. 6. The two pyrophosphate-binding sites. Hydrogen-bonding partners of the pyrophosphates as seen in the A- and B-view are shown. Labels A- and B- in front of the residues refer to the two monomers. The bond length in angstroms is given as a number. This figure was made with ISIS-DRAW.

such a role. In support of this finding, Walter *et al*. (1992) state that mutants of S.t.MalK in the corresponding Gln82 residue do not have significantly reduced ATPase activity. According to our structure, the nearby residues His95 and Tyr93 in T.l.MalK could both sense the presence of a phosphate.

Another hint of the functional competence of the observed dimer structure is provided by the evenly positive electrostatic surface potential in the surroundings of the nucleotide-binding site (data not shown). As both monomers contribute to the potential there, we interpret this as evidence that they are adjusted to each other in order to facilitate entrance of the nucleotide to its site in the interface.

Recently, W.Reenstra and colleagues (W.Wang, Z.He and W.Reenstra, unpublished data) identified two polypeptide segments of the nucleotide-binding domains of CFTR that are involved in interdomain interactions. Alignment of these segments with the MalK sequence shows that they both map into the T.l.MalK dimer interface, indicating a roughly similar dimeric association in both cases.

Interaction with MalFG and asymmetry of the MalK dimer

Hunke *et al*. (2000a) report that Ala85 of S.t.MalK is in the close neighbourhood of MalF and MalG. In T.l.MalK, the corresponding residue Ala91 is part of the 'lid' region that extends close to the bottom of the dimer structure. Furthermore, chimeric fusion proteins (Wilken *et al*., 1996) indicated that residues 89–140 in S.t.MalK are crucial for functional, high-affinity interaction with MalFG. In T.l.MalK, this segment maps to helices 2 and 3 as well as to the signature motif region. In subsequent studies, Schmees *et al*. (1999) have shown that mutations in the signature motif region fail to restore a functional transport complex. Recently, Hunke *et al*. (2000a) have identified

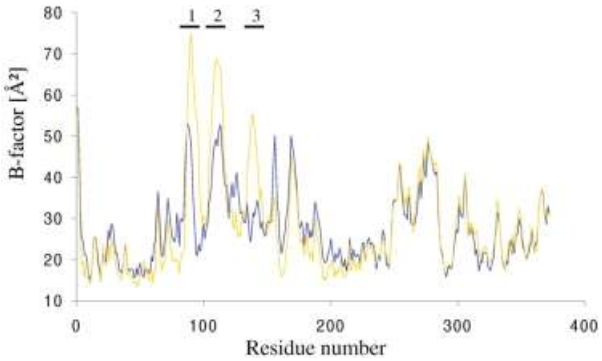

Fig. 7. *B*-factors of the C_α atoms of the A- (yellow) and B- (blue) monomer of T.l.MalK. Regions of high asymmetry are marked by bars and labelled with numbers. The A-chain is significantly more disordered in the 'lid 'region (1), the loop between helices 2 and 3 (2) and the signature motif region (3). The regulatory domains have fairly similar *B*-factors.

two valines mapping to helix 3 in T.l.MalK that cross-link with MalFG, one of them in an ATP-dependent manner. Helices 2 and 3 are located in the peripheral part of the dimer interface (Figure 1B) and are among the most asymmetric structural elements in T.l.MalK. Furthermore, asymmetric *B*-factors are found in the loop between them and in the signature motif region, which is located at the very bottom of the dimer (Figure 2).

These findings strongly suggest that the helices and the signature motif region at the bottom of the dimer structure are involved in complex formation with the translocation pore MalFG (Figures 1A and 2). The docking of a MalE–maltose complex to the periplasmic surface must somehow trigger the ATPase cycle of MalK. Indeed, studies of mutations of S.t.MalK P160L and D165N in the D-loop (Hunke *et al*., 2000b) have shown that residues at the bottom of MalK, remote from the ATP site, can be

incompatible with ATP hydrolysis. Such interference of a mutation with hydrolysis can be dependent upon interaction with MalFG, as the L86F mutation of S.t.MalK (Hunke *et al*., 2000b) has shown. This residue is part of the 'lid' region and, in T.l.MalK, it precedes A-Tyr93, which approaches a pyrophosphate to within hydrogen-bonding distance in the B-molecule.

At present, the functional relevance of the broken 2-fold symmetry in the structure of the T.l.MalK dimer remains elusive, and three alternative explanations are available. (i) Crystal lattice forces may have deformed the dimer into an artificial asymmetry. In view of the observed deviations from 2-fold symmetry, this explanation appears to be unlikely, as important deviations are not near the crystal contacts, and the crystal contacts themselves as well as the differences in contacts between the two monomers are rather weak. (ii) The conformation of each monomer may represent one close-to-native structure, and the two homodimers formed from them would be perfectly symmetrical. This argument might possibly apply to the free (uncomplexed) MalK dimer. (iii) The observed structure may be close to one conformation of the MalK dimer complexed with the heterodimeric transmembrane translocation pore MalFG, which can be expected to exert asymmetric forces on the former. As the structure of the F_1,F_0-ATPase has taught us, a deviation from symmetry may be an essential feature of a functional ATPase. Furthermore, large domain movements are a common feature of all ATPases and kinases. Thus, the deviation in the symmetry of the MalK dimer predicts further movements during the transport cycle.

Moreover, indirect evidence for further conformations different from those reported here exists. His192 of E.c.MalK, for example, is known to be critical for maltose transport and ATP hydrolysis (Davidson and Sharma, 1997). In the dimer structure of T.l.MalK, the side chain of the corresponding residue His198 is ~8 Å away from the nearest β-phosphate oxygen. Even if a nucleoside triphosphate would be bound, its γ-phosphate would be too far away to hydrogen-bond with the histidine in the present conformations. With an interspersed water molecule as in the HisP structure (Hung *et al*., 1998) and an altered side chain conformation, a direct contact could be formed.

We recently found another conformation of T.l.MalK in a new crystal form that possesses the same basic dimer structure but with perfect 2-fold symmetry (unpublished data).

MalK as a donor and acceptor of regulatory signals. Are there common features with other nucleotide-hydrolysing enzymes involved in signal transduction?

Each strand of the parallel sheet of the middle layer is followed by a loop and a helix, a pattern that may represent a functional module serving as a 'phosphate sensor' (Vale, 1996). In accordance with a modular structure, conserved regions of residues are found in each of them (Figure 2). Strand 3 followed by the P-loop and helix 1 contain the Walker-A motif. Strand 9 and the subsequent loop contain the switch motif. Strand 8 and the subsequent loop contain the Walker-B motif and the D-loop motif. Strand 7 is followed by an extended loop region, which contains a weakly conserved region that has attracted little attention so far. This 'lid' region is followed by helices 2 and 4, which are placed in the interface of the dimer structure. The 'lid' regions of the two monomers approach each other in the interface so that the backbone C_α atoms have a closest distance of 8.4 Å near residue Gln88, which is highly conserved in ABC-type ATPases. GTPases, myosins and kinesins possess the same arrangement of three β-strands and loops with a characteristic Walker-A, switch and Walker-B motif, indicating that they establish similar mechanisms in all of them (Vale, 1996). They discriminate between bound nucleoside triphosphate and bound nucleoside diphosphate-P_i and induce a conformational transition when the β–γ-phosphate bond is cleaved. In the bacterial elongation factor EF-Tu, for example, a C-terminal domain is relocated, apparently serving as a switch between docking and release of the ligand aminoacyl-tRNA.

When the ABC-type ATPases are compared with GTPases, the Walker-A region is conserved rather well, whereas the switch and the Walker-B regions are not conserved. Moreover, strand 8 containing most of the Walker-B motif is oriented oppositely. In spite of these differences, it is tempting to assign a common function to each of these modules, which would mean that in T.l.MalK the transition from the ATP ligand to the ADP-P_i ligand causes a relocation of the regulatory domain relative to the ATPase domain, similar to that in EF-Tu. Such a conformational transition may trigger a signal by changing the affinity for effector molecules. In *T.litoralis*, the effector molecules interacting with the regulatory domain and the regulatory purposes are unknown. As the regulatory domains of E.c.MalK and T.l.MalK appear to belong to the same fold, the structure of the latter can be used as a model to discuss known facts about regulatory functions of E.c.MalK. In *E.coli*, a conformational transition during the functional cycle apparently abolishes transiently the high binding affinity of the regulatory domain for the transcriptional activator MalT (Panagiotidis *et al*., 1998). T.l.MalK and E.c.MalK may thus possess features of G-proteins.

E.c.MalK can not only send but can also accept regulatory signals. Upon interaction with another effector, unphosphorylated $EIIA^{Glc}$, maltose uptake is inhibited (Vandervlag and Postma, 1995). It appears feasible that one of the conformations in the functional cycle of *E.coli* MalK possesses high affinity for this effector and that the ATPase cycle is blocked upon binding so that the uptake of maltose is reduced.

Mutants highlight the mechanistic connection between the regulatory domain and the ATPase domain. E306K of purified S.t.MalK (Hunke *et al*., 2000b) in the conserved region at the end of strand 17 shows a significantly reduced ATPase activity compared with the wild type without affecting the repressor-like activity associated with MalT binding. Other mutations nearby have been shown to abolish the repressor function (G302D in E.c.MalK; Kühnau *et al*., 1991). This indicates that both sites for effector interactions and sites mediating repercussions on transport by $MalFGK_2$ may reside in the regulatory domains.

Conversely, mutations in the ATPase domain can lock the regulatory domain in a MalT-binding conformation. Kühnau *et al*. (1991) have shown that the mutation G137A

in the signature motif region of E.c.MalK retains ATP binding but abolishes ATP hydrolysis and, by tight binding of MalT, establishes repression of transcription, leading to the descriptive term 'super-repressor mutation'.

It should be noted again that in *T.litoralis* neither a transcriptional activator similar to MalT nor a phosphotransferase system with a subunit similar to $EIIA^{Glc}$ is known.

Hypothetical mechanistic outlines of maltose transport

The major part of the binding energy of two ATP molecules (in T.l.MalK, K_M = 155 μM; Greller *et al*., 1999) may be stored as conformational strain in the transporter. Indeed, ATP binding was shown to induce a conformational transition. In HisP, Tyr16 in strand 1 stacks on the adenine group. This may pull the antiparallel sheet closer to the centre of the ATPase domain and cause the observed reduction in trypsin accessibility of S.t.MalK in this region at the top of the dimer structure (Schneider *et al*., 1994). Moreover, in the presence of ATP, a reduction of the distance between the Ala85 residues in S.t.MalK (Hunke *et al*., 2000a) was observed.

When MalE–maltose docks to the periplasmic binding site, the binding energy (K_D ~1 μM; Davidson *et al*., 1992) may cause a conformational transition of MalFG, which may involve the cytoplasmically exposed domains. This could trigger release of the stored strain energy. Part of the released energy may deform MalE, abolishing its affinity for maltose. Simultaneously, another part of the energy may be used to convert the MalFG transmembrane domain against the lipid–protein interfacial tension into an open water channel. Maltose could then diffuse freely or in a surface-absorbed state through the channel.

Furthermore, the transition to the open channel conformation would also change the conformation of the regulatory domain, i.e. switch it to a 'signalling-competent state', a mechanism reminiscent of G-protein signalling. This could mean release of the transcriptional activator MalT from E.c.MalK, which is ~100 times more abundant than MalT, during the open channel conformation.

Simultaneously with the channel opening, MalK may be converted into a slow ATPase, which eventually leads to ATP hydrolysis and channel closure. Thus, after some preset time that is long enough for the diffusion of maltose through the translocation pore to the cytoplasm, cooperative ATP hydrolysis (Davidson *et al*., 1996) could take place. The regulatory domains would then lose their signalling competence and the channel would close.

The proposed hypothetical model is in accord with available genetic and biochemical data and contains some features of a proposed mechanism for active transport through outer membranes (Ferguson *et al*., 1998). All mechanistic details mediated by the protein are unknown. The deviation from 2-fold symmetry of the dimer structure in the 'lid' region and the apposition of the conserved glutamine residues of both monomers together may be relevant features. If the glutamine residues would form an intermolecular hydrogen bond in a hydrophobic environment, the positions of other pairs of symmetry-related and functionally important residues in the 'lid' of both monomers may be restricted and correlated. This could establish a coordination of catalytic events in both monomers, as observed in the NBD domains of P-glycoprotein (Senior *et al*., 1995; Senior and Bhagat, 1998).

The observed apposition of Ala85 in E.c.MalK with residues of MalF and MalG may mean that interactions of the 'lid' with the translocation pore are also involved in the transport cycle.

Materials and methods

Culture conditions

Escherichia coli strain BL21 (Studier and Moffatt, 1986) was transformed with the plasmid pGG200 constructed analogous to pGG100 (Greller *et al*., 1999) selecting for ampicillin resistance. The transformants were pooled and aliquoted, frozen in liquid nitrogen and stored at –70°C. These aliquots were used to inoculate overnight cultures subsequently used for large-scale cultures. The fermentation was performed according to Riesenberg *et al*. (1991) in a Biostat C benchtop fermenter (Braun, Melsungen, Germany) equipped with a 15 l water-jacketed stainless steel vessel and microprocessor control of pH, dissolved oxygen, agitation, temperature and nutrient feed. The temperature was kept at 28°C. The medium was as described by Riesenberg *et al*. (1991), containing additional NZA medium [10 g of NZ-amine A (Sheffield Products Inc., UK), 5 g of yeast extract and 7.5 g of NaCl per litre]. To inoculate the fermenter, 10 ml of cells grown in tubs in NZA medium containing 200 mg of ampicillin/l were added. After the culture reached an optical density (OD) at 578 nm (A578) of 50, expression of the plasmid-encoded *mal*K gene was induced by adding isopropyl-β-D-thiogalactopyranoside (IPTG) to a final concentration of 0.1 mM. Four hours later, at an OD of 100, the fermenter was cooled to 10°C prior to harvesting. The culture was harvested by centrifugation at 5000 *g* for 30 min at 4°C, frozen in liquid nitrogen and stored at –70°C.

Purification of His_6-MalK

Fifty grams cell wet weight of the pellet from BL21-induced cells containing plasmid pGG200 were resuspended in 100 ml of buffer 1 (50 mM Tris–HCl pH 7.5, 5 mM $MgCl_2$ containing 500 mM NaCl), ruptured in a French pressure cell at 16 000 p.s.i. and centrifuged for 15 min at 19 000 *g*. The supernatant was heated to 70°C for 20 min. After centrifugation of the precipitated proteins (30 min at 19 000 *g*), imidazole was added to the supernatant to a final concentration of 20 mM. The solution was loaded onto a 4 ml bed volume Ni^{2+}-NTA–agarose column (Qiagen, Hilden, Germany) equilibrated with the same buffer. After washing the column with 80 ml of buffer 1 supplemented with 20 mM imidazole, MalK was eluted with buffer 1 containing 200 mM imidazole. MalK-containing fractions (10 ml) were pooled and loaded onto an 8 ml bed volume Reactive Red agarose 120 (3000-CL) column (Sigma, Munich, Germany) equilibrated with buffer 1. The column was washed with five bed volumes of buffer 1. MalK was eluted with buffer 1 containing 2 M NaCl. MalK-containing fractions (30 ml) were pooled. A Centricon 30 concentrator (Amicon, Witten, Germany) was used to concentrate to 5 mg/ml and to change the buffer to 50 mM Tris–HCl pH 7.5, 5 mM $MgCl_2$ and 200 mM NaCl. The total yield of purified His_6-T.l.MalK from 50 g cell wet weight was routinely between 60 and 100 mg. The enzyme was stored at 4°C without loss of activity.

Crystallization and structure solution

Crystals were grown at 18°C using the hanging drop vapour diffusion method with the aid of Hampton Research screening solutions (Hampton Research, Laguna Niguel, USA). The crystallization buffer contained 2 M ammonium sulfate, 5% dioxane and 100 mM Tris pH 8.5. Drops were prepared by mixing 5 μl of MalK solution (5 mg/ml) with 5 μl of crystallization buffer containing 1 mM ADP. Crystals appeared after 3 weeks. For data collection at 100 K, the crystals were soaked for 5 min in the crystallization buffer supplemented with 15% glycerol. The crystals were frozen rapidly and stored in liquid nitrogen.

Heavy atom derivatives were obtained by adding 1 μl of a 10 mM $HgCl_2$ solution to the crystallization drop. The crystals were incubated for 16 h in the crystallization buffer containing the heavy atom salt, and then frozen in liquid nitrogen.

Data sets were measured using synchrotron X-ray sources at 100 K using Mar345 and Mar CCD image plate detectors (Table I). Native crystals diffracted to better than 1.9 Å at beamline BW7B (DESY/EMBL, Hamburg, Germany). Four data sets of an $HgCl_2$-soaked crystal at

Table II. Statistics of the MalK structure

Protein atoms	5878
Ligand atoms	35
Solvent atoms	447
Resolution range (Å)	50–1.9
R-factor (%)	21.1
R_{free} (%)	24.8
R.m.s. bond length deviations (Å)	0.007
R.m.s. bond angles deviations (°)	1.306
Ramachandran plot	
most favoured regions (%)	90.8
additionally allowed regions (%)	8.9
generously allowed regions (%)	0.3
disallowed regions (%)	0.0

different wavelengths were collected at beamline BW7A (DESY/EMBL, Hamburg) for phase calculation using MAD.

The data were processed using the XDS program suite (Kabsch, 1993). The crystals grow in space group $P2_12_12$ (a = 190.72 Å, b = 65.70 Å, c = 77.91 Å) with two molecules per asymmetric unit.

Two heavy atom sites were found using the program SOLVE (Terwilliger and Berendzen, 1999). Further refinement of the heavy atom sites was performed using SHARP (de la Fortelle and Bricogne, 1997). The resulting electron density map was solvent flattened using the program SOLOMON (CCP4, 1994; Abrahams and Leslie, 1996), and the resulting phases were used for automated model building using the ARP/wARP (Lamzin and Wilson, 1993) program suite.

Further refinement was performed using individual *B*-factor refinement, torsion angle dynamics by slow cooling the model after heating to 2000 K and energy minimization in CNS (Brünger *et al*., 1998). Grouped occupancy refinement was performed for the pyrophosphate. Modelling was performed using O (Jones *et al*., 1991). The quality of the structure (Table II) was analysed using PROCHECK (Laskowski *et al*., 1993) and WHATIF (Vriend, 1990). The final model comprises residues 1–372 of the native form of MalK (but not the N-terminal affinity tag MRGSHHHHHHTDP), two pyrophosphate molecules, three dioxane molecules and 447 solvent molecules.

The coordinates have been deposited in the Protein Data Bank (accession No. 1G29).

Acknowledgements

We are grateful to the staff of EMBL/DESY for their help during data collection and to Drs Michael Ehrmann and Martin Hug for critical reading of the manuscript and useful discussions. This work was supported by the Deutsche Forschungsgemeinschaft and the Fonds der Chemischen Industrie.

References

Abrahams,J.P. and Leslie,A.G.W. (1996) Methods used in the structure determination of F_1-ATPase. *Acta Crystallogr. D*, **52**, 30–42.

Armstrong,S., Tabernero,L., Zhang,H., Hermodson,M. and Stauffacher,C. (1998) Powering the ABC transporter: the 2.5 Å crystallographic structure of the ABC domain of RbsA. *Pediatr. Pulmonol.*, **7**, 91–92.

Bavoil,P., Hofnung,M. and Nikaido,H. (1980) Identification of a cytoplasmic membrane-associated component of the maltose transport system of *E.coli*. *J. Biol. Chem.*, **255**, 8366–8369.

Boos,W. and Lucht,J.M. (1996) Periplasmic binding-protein dependent ABC transporters. In Neidhard,F.C. *et al*. (eds), *Escherichia coli and Salmonella typhimurium: Cellular and Molecular Biology*. 2nd edn, Vol. 1. American Society of Microbiology, Washington, DC, pp. 1175–1209.

Boos,W. and Shuman,H.A. (1998) The maltose/maltodextrin system of *Escherichia coli*; transport, metabolism and regulation. *Microbiol. Mol. Biol. Rev.*, **62**, 204–229.

Brünger,A.T. *et al*. (1998) Crystallography and NMR system: a new software suite for macromolecular structure determination. *Acta Crystallogr. D*, **54**, 905–921.

CCP4 (1994) The CCP4 suite: programs for protein crystallography. *Acta Crystallogr. D*, **50**, 760–763.

Davidson,A.L. and Nikaido,H. (1991) Purification and characterization of the membrane-associated components of the maltose transport system from *Escherichia coli*. *J. Biol. Chem.*, **266**, 8946–8951.

Davidson,A.L. and Sharma,S. (1997) Mutation of a single MalK subunit severely impairs maltose transport activity in *Escherichia coli*. *J. Bacteriol.*, **179**, 5458–5464.

Davidson,A.L., Shuman,H.A. and Nikaido,H. (1992) Mechanism of maltose transport in *Escherichia coli*: transmembrane signaling by periplasmic binding proteins. *Proc. Natl Acad. Sci. USA*, **89**, 2360–2364.

Davidson,A.L., Laghaeian,S.S. and Mannering,D.E. (1996) The maltose transport system of *Escherichia coli* displays positive cooperativity in ATP hydrolysis. *J. Biol. Chem.*, **271**, 4858–4863.

Dean,D.A., Reizer,J., Nikaido,H. and Saier,M. (1990) Regulation of the maltose transport system of *Escherichia coli* by the glucose-specific enzyme III of the phosphoenolpyruvate–sugar phosphotransferase system. Characterization of inducer-exclusion-resistant mutants and reconstitution of inducer exclusion in proteoliposomes. *J. Biol. Chem.*, **265**, 21005–21010.

de la Fortelle,E. and Bricogne,G. (1997) Maximum-likelihood heavy-atom parameter refinement for multiple isomorphous replacement and multiwavelength anomalous diffraction methods. *Methods Enzymol.*, **276**, 472–494.

Diederichs,K. and Karplus,P.A. (1997) Improved *R*-factors for diffraction analysis in macromolecular crystallography. *Nature Struct. Biol.*, **4**, 269–275.

Ehrmann,M.,R., Ehrle,E., Hofmann,E., Boos,W. and Schlösser,A. (1998) The ATP maltose transporter. *Mol. Microbiol.*, **29**, 685–694.

Ferguson,A.D., Hofmann,E., Coulton,J.W., Diederichs,K. and Welte,W. (1998) Siderophore-mediated iron transport: crystal structure of FhuA with bound lipopolysaccharide. *Science*, **282**, 2215–2220.

Greller,G., Horlacher,R., DiRuggiero,J. and Boos,W. (1999) Molecular and biochemical analysis of MalK, the ATP-hydrolyzing subunit of the trehalose maltose transport system of the hyperthermophilic archaeon *Thermococcus litoralis*. *J. Biol. Chem.*, **274**, 20259–20264.

Herrmann,A., Schlösser,A., Schmid,R. and Schneider,E. (1996) Biochemical identification of a lipoprotein with maltose-binding activity in the thermoacidophilic Gram-positive bacterium *Alicyclobacillus acidocaldarius*. *Res. Microbiol.*, **147**, 733–737.

Holland,B. and Blight,M.A. (1999) ABC-ATPases, adaptable energy generators fuelling transmembrane movement of a variety of molecules in organisms from bacteria to humans. *J. Mol. Biol.*, **293**, 381–399.

Holm,L. and Sander,C. (1993) Protein structure comparison by alignment of distance matrices. *J. Mol. Biol.*, **233**, 123–138.

Hopfner,K.-P., Karcher,A., Shin,D.S., Craig,L., Arthur,L.M., Carney,J.P. and Tainer,J.A. (2000) Structural biology of Rad50 ATPase: ATP-driven conformational control in DNA double-strand break repair and the ABC-ATPase superfamily. *Cell*, **101**, 789–800.

Horlacher,R., Xavier,K.B., Santos,H., DiRuggiero,J., Kossmann,M. and Boos,W. (1998) Archaeal binding protein-dependent ABC transporter: molecular and biochemical analysis of the trehalose/maltose transport system of the hyperthermophilic archaeon *Thermococcus litoralis*. *J. Bacteriol.*, **180**, 680–689.

Hung,L.-W., Wang,I.X., Nikaido,K., Liu,P.-Q., Ames,G.F.-L. and Kim,S.-H. (1998) Crystal structure of the ATP-binding subunit of an ABC transporter. *Nature*, **396**, 703–707.

Hunke,S., Mourez,M., Jéhanno,M., Dassa,E. and Schneider,E. (2000a) ATP modulates subunit–subunit interactions in an ATP-binding-cassette transporter ($MalFGK_2$) determined by site-directed chemical crosslinking. *J. Biol. Chem.*, **275**, 15526–15534.

Hunke,S., Landmesser,H. and Schneider,E. (2000b) Novel missense mutations that affect the transport function of MalK, the ATP-binding-cassette subunit of the *Salmonella enterica* serovar *typhimurium* maltose transport system. *J. Bacteriol.*, **182**, 1432–1436.

Jones,T.A., Zou,J.Y., Cowan,S.W. and Kjeldgaard,M. (1991) Improved methods for building protein models in electron density maps and the location of errors in these models. *Acta Crystallogr. A*, **47**, 110–119.

Kabsch,W. (1993) Automatic processing of rotation diffraction data from crystals of initially unknown symmetry and cell constants. *J. Appl. Crystallogr.*, **26**, 795–800.

Kennedy,K.A. and Traxler,B. (1999) MalK forms a dimer independent of its assembly into the $MalFGK_2$ ATP-binding cassette transporter of *Escherichia coli*. *J. Biol. Chem.*, **274**, 6259–6264.

Kjeldgaard,M. and Nyborg,J. (1992) Refined structure of elongation factor EF-Tu from *Escherichia coli*. *J. Mol. Biol.*, **223**, 721–742.

Kraulis,P.J. (1991) MOLSCRIPT: a program to produce both detailed

and schematic plots of protein structures. *J. Appl. Crystallogr.*, **24**, 946–950.

Kühnau,S., Reyes,M., Sievertsen,A., Shuman,H.A. and Boos,W. (1991) The activities of the *Escherichia coli* MalK protein in maltose transport, regulation and inducer exclusion can be separated by mutations. *J. Bacteriol*., **173**, 2180–2186.

Lamzin,V.S. and Wilson,K.S. (1993) Automated refinement of protein models. *Acta Crystallogr. D*, **49**, 129–149.

Laskowski,R.A., MacArthur,M.W., Moss,D.S. and Thornton,J.M. (1993) PROCHECK: a program to check the stereochemical quality of protein structures. *J. Appl. Crystallogr.*, **26**, 283–291.

Linton,K.J. and Higgins,C.F. (1998) The *Escherichia coli* ATP-binding cassette (ABC) proteins. *Mol. Microbiol.*, **28**, 5–13.

Lippincott,J. and Traxler,B. (1997) MalFGK complex assembly and transport and regulatory characteristics of malK insertion mutants. *J. Bacteriol*., **179**, 1337–1343.

Morbach,S., Tebbe,S. and Schneider,E. (1993) The ATP-binding cassette (ABC) transporter for maltose/maltodextrins of *Salmonella typhimurium*. Characterization of the ATPase activity associated with the purified MalK subunit. *J. Biol. Chem.*, **268**, 18617–18621.

Mourez,M., Hofnung,M. and Dassa,E. (1997) Subunit interactions in ABC transporters: a conserved sequence in hydrophobic membrane proteins of periplasmic permeases defines an important site of interaction with the ATPase subunits. *EMBO J.*, **16**, 3066–3077.

Murzin,A.G. (1993) OB (oligonucleotide/oligosaccharide binding)-fold: common structural and functional solution for non-homologous sequences. *EMBO J.*, **12**, 861–867.

Nyborg,J., Nissen,P., Kjeldgaard,M., Thirup,S., Polekhina,G. and Clark,B.F.C. (1996) Structure of the ternary complex of EF-Tu: macromolecular mimicry in translation. *Trends Biochem. Sci.*, **21**, 81–82.

Panagiotidis,C.H., Reyes,M., Sievertsen,A., Boos,W. and Shuman,H.A. (1993) Characterization of the structural requirements for assembly and nucleotide binding of an ATP-binding cassette transporter—the maltose system of *Escherichia coli. J. Biol. Chem.*, **268**, 23685–23696.

Panagiotidis,C.H., Boos,W. and Shuman,H.A. (1998) The ATP-binding cassette subunit of the maltose transporter MalK antagonizes MalT, the activator of the *Escherichia coli mal* regulon. *Mol. Microbiol.*, **30**, 535–546.

Riesenberg,D., Schulz,V., Knorre,W.A., Pohl,H.D., Korz,D., Sanders, E.A., Ross,A. and Decker,W.D. (1991). High cell density cultivation of *Escherichia coli* at controlled specific growth rate. *J. Biotechnol.*, **20**, 17–27.

Sahm,K., Matuschek,M., Müller,H., Mitchell,W.J. and Bahl,H. (1996) Molecular analysis of the *amy* gene locus of *Thermoanaerobacterium thermosulfurigenes* EM1 encoding starch-degrading enzymes and a binding protein-dependent maltose transport system. *J. Bacteriol*., **178**, 1039–1046.

Schmees,G. and Schneider,E. (1998) Domain structure of the ATP-binding-cassette protein MalK of *Samonella typhimurium* as assessed by coexpressed half molecules and LacK′-′MalK chimeras. *J. Bacteriol*., **180**, 5299–5305.

Schmees,G., Stein,A., Hunke,S., Landmesser,H. and Schneider,E. (1999) Functional consequences of mutations in the conserved 'signature sequence' of the ATP-binding-cassette protein malK. *Eur. J. Biochem.*, **266**, 420–430.

Schmitt,E., Blanquet,S. and Mechulam,Y. (1996) Structure of crystalline *Escherichia coli* methionyl-tRNA$_f^{Met}$ formyltransferase: comparison with glycinamide ribonucleotide formyltransferase. *EMBO J.*, **15**, 4749–4758.

Schneider,E. and Hunke,S. (1998) ATP-binding cassette (ABC) transport systems: functional and structural aspects of the ATP-hydrolyzing subunits/domains. *FEMS Microbiol. Rev.*, **22**, 1–20.

Schneider,E., Wilken,S. and Schmid,R. (1994) Nucleotide-induced conformational changes of MalK, a bacterial ATP binding cassette transporter protein. *J. Biol. Chem.*, **269**, 20456–20461.

Senior,A.E. and Bhagat,S. (1998) P-glycoprotein shows strong catalytic cooperativity between the two nucleotide sites. *Biochemistry*, **37**, 831–836.

Senior,A.E., Al-Shawi,M.K. and Urbatsch,I.L. (1995) The catalytic cycle of P-glycoprotein. *FEBS Lett.*, **377**, 285–289.

Shuman,H.A. and Silhavy,T.J. (1981) Identification of the *malK* gene product. A peripheral membrane component of the *Escherichia coli* maltose transport system. *J. Biol. Chem.*, **256**, 560–562.

Studier,F.W. and Moffatt,B.A. (1986) Use of bacteriophage T7 RNA polymerase to direct selective high-level expression of cloned genes. *J. Mol. Biol.*, **189**, 113–130.

Terwilliger,T.C. and Berendzen,J. (1999) Automated structure solution for MIR and MAD. *Acta Crystallogr. D*, **55**, 849–861.

Vale,R.D. (1996) Switches, latches and amplifiers: common themes of G proteins and molecular motors. *J. Cell Biol.*, **135**, 291–302.

Vandervlag,J. and Postma,P.W. (1995) Regulation of glycerol and maltose uptake by the IIA(Glc)-like domain of II(Nag) of the phosphotransferase system in *Salmonella typhimurium* LT2. *Mol. Gen. Genet.*, **248**, 236–241.

Vriend,G. (1990) WHAT IF: a molecular modeling and drug design program. *J. Mol. Graphics*, **8**, 52–56.

Walter,C., Wilken,S. and Schneider,E. (1992) Characterization of site-directed mutations in conserved domains of MalK, a bacterial member of the ATP-binding cassette (ABC) family. *FEBS Lett.*, **303**, 41–44.

Wilken,S., Schmees,G. and Schneider,E. (1996) A putative helical domain in the MalK subunit of the ATP-binding cassette transport system for maltose of *Salmonella typhimurium* (MalFGK$_2$) is crucial for interaction with MalF and MalG. A study using the LacK protein of *Agrobacterium radiobacter* as a tool. *Mol. Microbiol.*, **22**, 655–666.

Xavier,K.B., Martins,L.O., Peist,R., Kossmann,M., Boss,W. and Santos,H. (1996) High-affinity maltose/trehalose transport system in the hyperthermophilic archaeon *Thermococcus litoralis*. *J. Bacteriol*., **178**, 4773–4777.

Received August 25, 2000; revised September 29, 2000; accepted October 2, 2000

Note added in proof

Ikuma and Welsh [*Proc. Natl Acad. Sci. USA* (2000), **97**, 8675–8680] have reported new data on channel opening in CFTR which are in accord with the model proposed here.